

Electronic Supporting Information

Modulation of Coordination Environment: A Convenient Approach to Tailor Magnetic Anisotropy in Seven Coordinate Co(II) Complexes

Mamon Dey, Snigdha Dutta, Bipul Sarma, Ramesh Ch. Deka and Nayanmoni Gogoi*
Department of Chemical Sciences, Tezpur University, Napaam-784028, Assam, India.
E-mail: ngogoi@tezu.ernet.in

Table of Contents:

General Experimental Remarks.....	S3
Synthesis of [Co(dapbh-H ₂)(SCN) ₂].3H ₂ O (1).....	S3
Synthesis of [Co(dapbh)(H ₂ O) ₂] (2).....	S3
X-Ray Diffraction Studies.....	S4
Table S1: Crystallographic data for 1 and 2	S5
Table S2. Selected bond lengths [Å] for 1 and 2	S5
Table S3. Selected bond angles [°] for for 1 and 2	S6
Table S4. Comparison of bond lengths [Å] in 1 and 2 with two other reported Co-dapbhH ₂ complexes.....	S6
Figure S1. Hydrogen bonding network present in 1	S7
Figure S2. Hydrogen bonding network present in 2	S7
Figure S3. Temperature dependence of χ_M curve for 1	S8
Figure S4. Variation of $1/\chi_M$ against temperature for 1	S8
Figure S5. Temperature dependence of χ_M curve for 2	S9
Figure S6. Variation of $1/\chi_M$ against temperature for 2	S9
Figure S7. Reduced magnetization M versus HT^{-1} plot of 1	S10
Figure S8. Reduced magnetization M versus HT^{-1} plot of 2	S10
References	S11

General Experimental Remarks:

Materials and Methods. Starting materials were procured from commercial sources and used as received. Solvents were purified by conventional techniques and distilled prior to use. Elemental analyses were performed on a Perkin Elmer Model PR 2400 Series II Elemental Analyzer. Infrared spectra were recorded on a Nicolet Impact I-410 FT-IR spectrometer as KBr diluted discs. Magnetic susceptibility data were collected on microcrystalline samples over a 2-300 K temperature range with an applied field of 500 Oe using a MPMS Squid magnetometer. Magnetization studies were performed between 0-5 T at 2K. 2, 6-diacetylpyridinebis(benzoic acid hydrazone), $[\text{Co}(\text{dapbh-H}_2)(\text{H}_2\text{O})(\text{NO}_3)]\text{NO}_3$ and $[\text{Ni}(\text{N}_3)_2(\text{dpa})_2(\text{N}_3)_2]\cdot\text{H}_2\text{O}$ (dpa=2,2'-dipyridyl amine) was prepared following a published procedure.¹⁻³

Synthesis of $[\text{Co}(\text{dapbh-H}_2)(\text{SCN})_2]\cdot 3\text{H}_2\text{O}$ (1):

To a methanolic solution of $[\text{Co}(\text{dapbh-H}_2)(\text{H}_2\text{O})(\text{NO}_3)]\text{NO}_3$ (0.015 mmol, 0.010 g) was added a solution of KSCN (0.0315 mmol, 0.003 g) in 10 mL H_2O . The reaction mixture was stirred at room temperature for an hour during which the color of the solution turned from bright orange to pale orange. The reaction mixture was filtered and the filtrate was kept undisturbed for slow evaporation at room temperature. Brown needle shaped crystals were observed after a week. The mother liquor was decanted and crystals were washed with minimum amount of ethanol and then dried with diethyl ether. Yield: 0.007 g (76 % based on Co) Found: C, 47.91%; H, 4.31%; N, 16.12%. $\text{C}_{25}\text{H}_{27}\text{N}_7\text{O}_5\text{S}_2\text{Co}$ requires C, 47.79%; H, 4.33%; N, 15.60%. IR (KBr, cm^{-1}): 3558(br), 2074(s), 1620(s), 1520(m), 1444(m), 1380(w), 1283(s), 1178(s), 1078(m), 1078(w), 801(m), 714(m), 466(w).

Synthesis of $[\text{Co}(\text{dapbh})(\text{H}_2\text{O})_2]$ (2):

To a solution of $[\text{Co}(\text{dapb-H}_2)(\text{NO}_3)(\text{H}_2\text{O})]\text{NO}_3$ (0.015 mmol, 0.010 g) in 20 mL of ethanol, $[\text{Ni}(\text{N}_3)_2(\text{dpa})_2(\text{N}_3)_2]\cdot\text{H}_2\text{O}$ (dpa=2,2'-dipyridyl amine) (0.027 mmol, 0.013 g) was added and heated for an hour. The reaction mixture was cooled, filtered and the filtrate was kept undisturbed for slow evaporation at room temperature. Bright orange needle-like crystals were observed after 24 hours. The mother liquor was discarded and crystals were washed with ethanol followed by diethyl ether and then air dried. Yield: 0.007 g (81 % based on Co) Found: C, 56.13%; H, 4.71%; N, 14.55%. $\text{C}_{23}\text{H}_{23}\text{N}_5\text{O}_4\text{Co}$ requires C, 56.11%; H, 4.71%; N,

14.22%. IR (KBr, cm^{-1}): 3251(br), 1677(w), 1579(m), 1498(s), 1411(w), 1371(s), 1163(m), 1046(m), 992(w), 903(w), 796(m), 690(m), 422(w).

X-Ray Diffraction Studies.

Suitable single crystals of all the compounds were obtained directly from the reaction mixtures, were used for diffraction measurements. The diffraction data for the compounds were collected on a Bruker APEX-II CCD diffractometer using $\text{MoK}\alpha$ radiation ($\lambda=0.71073 \text{ \AA}$) using φ and ω scans of narrow (0.5°) frames at 90-100K. All the structures were solved by direct methods using SHELXL-97⁴ as implemented in the WinGX program system. Anisotropic refinement was executed on all non-hydrogen atoms. The aliphatic and aromatic hydrogen atoms were placed on calculated positions but were allowed to ride on their parent atoms during subsequent cycles of refinements. Positions of N-H and O-H hydrogen atoms were located on a difference fourier map and allowed to ride on their parent atoms during subsequent cycles of refinements. Crystallographic data (excluding structure factors) for the structure in this paper have been deposited with the Cambridge Crystallographic Data Centre, CCDC, 12 Union Road, Cambridge CB21EZ, UK. Copies of the data can be obtained free of charge on quoting the depository number CCDC 1421271 (**1**) and CCDC 1421272 (**2**) (Fax: +44-1223-336-033; E-Mail: deposit@ccdc.cam.ac.uk, <http://www.ccdc.cam.ac.uk>).

Computational Details

DFT level single point calculations were carried on the experimental structures using the ORCA program package.⁵ For the transition metal centre, i.e. Co(II) ion Stuttgart/Dresden ECPs (SDD) basis sets and the def2-TZVP Ahlrichs basis set for Coulomb fitting, i.e. def2-TZVP/J is used.² For all other atoms def2 basis set of the Ahlrich group along with TZVP basis set was used.³ A hybrid DFT functional B3LYP was used for all DFT calculations.⁴ Since both the complexes are open shell systems with spin multiplicity greater than 1, unrestricted Kohn-Sham (UKS) wavefunction was used. To be on the safe side of SCF convergence of DFT calculation, NoFinalGrid keyword and spin-orbit operator based on mean-field approach are applied. For calculating contribution of spin-orbit coupling to the D tensor, Coupled-Perturbed (CP) method is used as it uses revised pre-factors for the spin-flip terms. Meanwhile for evaluating spin-spin contribution to D tensor, Breit-Pauli type operator is used along with canonical orbitals for the spin-density of the system.

Table S1: Crystallographic data for **1** and **2**.

Complex	1	2
CCDC Number	1421271	1421272
Empirical formula	C ₂₅ H ₂₁ CoN ₇ O ₅ S ₂	C ₂₃ H ₂₁ CoN ₅ O ₄
Formula weight	622.56	490.38
CCDC	1421271	1421272
Temperature/K	100	100
Crystal system	Orthorhombic	Orthorhombic
Space group	<i>P2₁2₁2₁</i>	<i>Cmc2₁</i>
a/Å	10.692 (2)	26.0390 (11)
b/Å	11.464 (2)	11.4044 (5)
c/Å	24.031 (2)	7.3288 (4)
α/°	90.00	90.00
β/°	90.00	90.00
γ/°	90.00	90.00
Volume/Å ³	2945.6 (10)	2176.25(18)
Z	4	4
ρ _{calc} g cm ⁻³	1.404	1.497
μ/mm ⁻¹	0.771	0.830
Crystal size, mm ³	0.25x0.17x0.11	0.32x0.08x0.06
F(000)	1276.0	1012.0
Reflections collected	5758	1815
Independent reflections	5193	1631
Data/parameters	370	162
Goodness-of-fit on F ²	1.100	1.209
Final R indexes [<i>I</i> ≥ 2σ (<i>I</i>)]	R1 = 0.0370, wR2 = 0.0938	R1 = 0.0340, wR2 = 0.0900
Final R indexes [all data]	R1 = 0.0443, wR2 = 0.1070	R1 = 0.0432, wR2 = 0.1232

Table S2. Selected bond lengths [Å] for **1** and **2**.

	1	2	
Co1-N1	2.187 (2)	Co1-N1	2.179 (4)
Co1-N2	2.190 (2)	Co1-N2	2.187 (3)
Co1-N4	2.200 (2)	Co1-N1	2.179 (4)
Co1-O1	2.302 (2)	Co1-O1	2.260 (2)
Co1-O2	2.228 (2)	Co1-O1	2.260 (2)
N2-N3	1.379 (3)	N1-N3	1.379 (4)
N4-N5	1.374 (3)	N1-N3	1.379 (4)

Table S3. Selected bond angles [°] for for **1** and **2**.

1		2	
N1-Co1-N2	70.8 (9)	N1-Co1-N2	70.8 (8)
N1-Co1-N4	70.3 (9)	N2-Co1-O4	95.7 (3)
N1-Co1-N7	91.2 (1)	N2-Co1-O3	89.1 (3)
N1-Co1-N6	89.2 (1)	N2-Co1-O1	140.1 (6)
N2-Co1-O1	70.0 (9)	O3-Co1-O1	88.7 (1)
N4-Co1-O2	147.2 (9)	O4-Co1-O1	87.5 (1)
O1-Co1-O2	77.4 (8)	O4-Co1-O3	175.2 (1)
C1-N1-Co1	119.3 (2)	C9-N1-Co1	121.9 (2)
C7-N2-N3	120.2 (2)	C9-N1-N3	117.2 (3)

Table S4. Comparison of bond lengths [Å] in **1** and **2** with two other reported Co-dapbhH₂ complexes.

	1	2	[Co(dapbH ₂)(H ₂ O)(NO ₃)]NO ₃	[Co(dapb)(im) ₂]
Co1-N(pyridine)	2.1873 (3)	2.1792 (1)	2.195	2.2112 (2)
Co1-N(imine)	2.2004 (4)	2.1871 (1)	2.190	2.2161 (2)
Co1-N(imine)	2.1901 (3)	2.1871 (1)	2.203	2.2161 (2)
Co1-O(equatorial)	2.3022 (4)	2.2600 (1)	2.150	2.2704 (1)
Co1-O(equatorial)	2.2279 (4)	2.2600 (1)	2.229	2.2704 (1)
Co1-N/O (axial)	2.1203 (4)	2.1194 (1)	2.114	2.1317 (2)
Co1-N/O (axial)	2.0787 (4)	2.0966 (1)	2.127	2.1317 (2)

Table S5: Decomposed excitations (in cm⁻¹) contributing towards spin-orbit coupling D_{SOC} calculated by DFT.

Complexes	D _{SOC}	$\alpha \rightarrow \alpha$ (SOMO \rightarrow VMO)	$\beta \rightarrow \beta$ (DOMO \rightarrow SOMO)	$\alpha \rightarrow \beta^*$ (SOMO \rightarrow SOMO)	$\beta \rightarrow \beta$ (DOMO \rightarrow VMO)
1	12.353	0.039	9.132	3.228	-0.047
2	10.251	1.196	5.981	4.203	-1.128

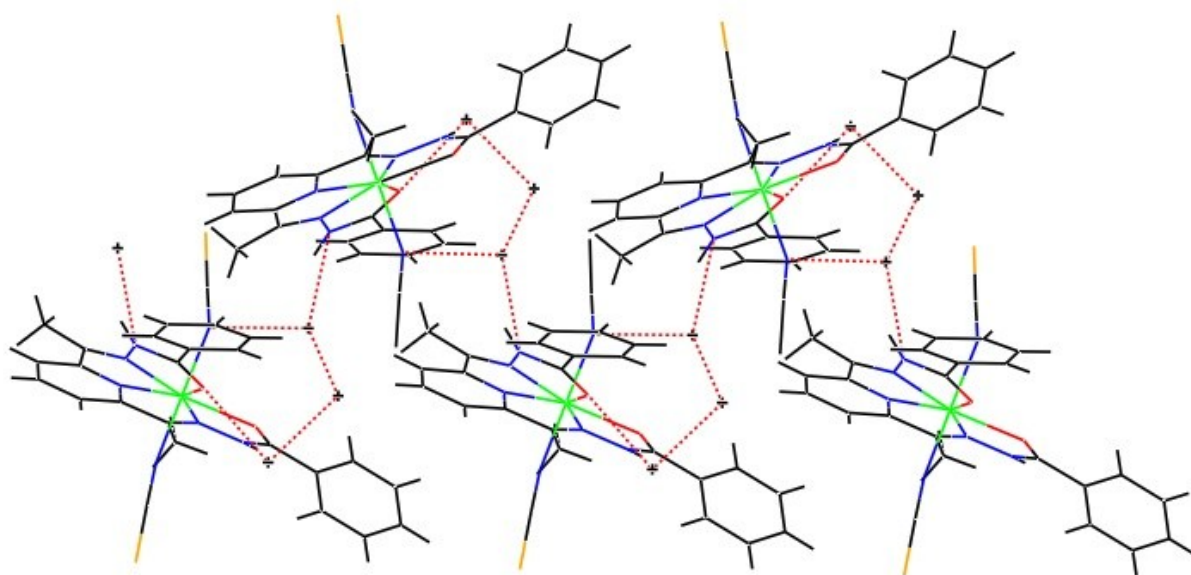


Figure S1. Helical one dimensional hydrogen bonding network present in **1**.

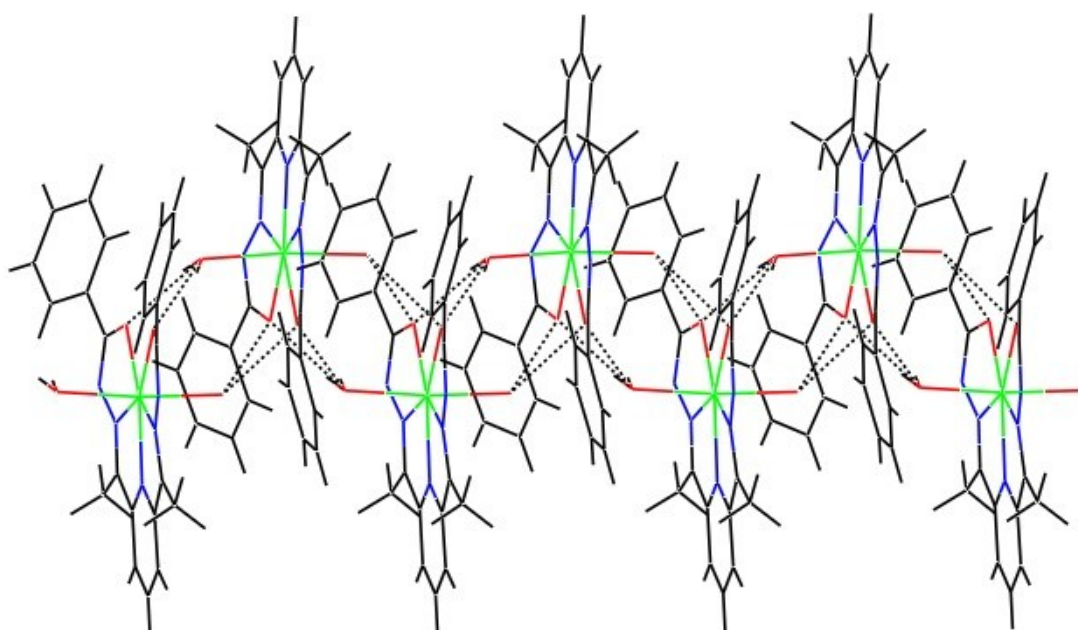


Figure S2. Zig-zag one dimensional hydrogen bonding network present in **2**.

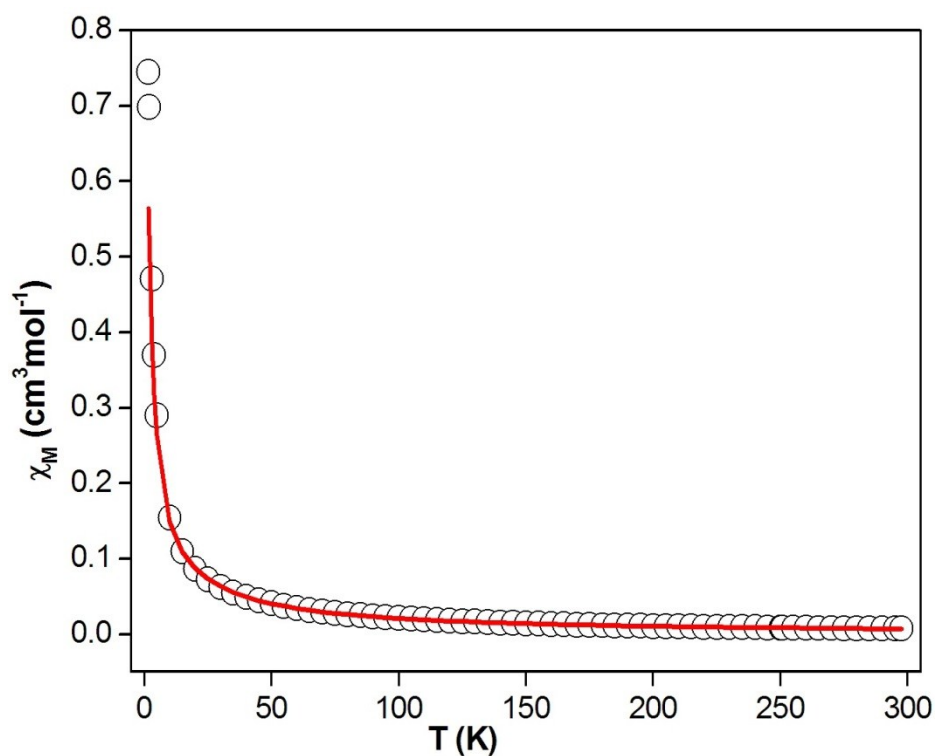


Figure S3. Temperature dependence of χ_M curve for **1**. Circles represent experimental value and the solid line represents the best fit obtained by using PHI program.

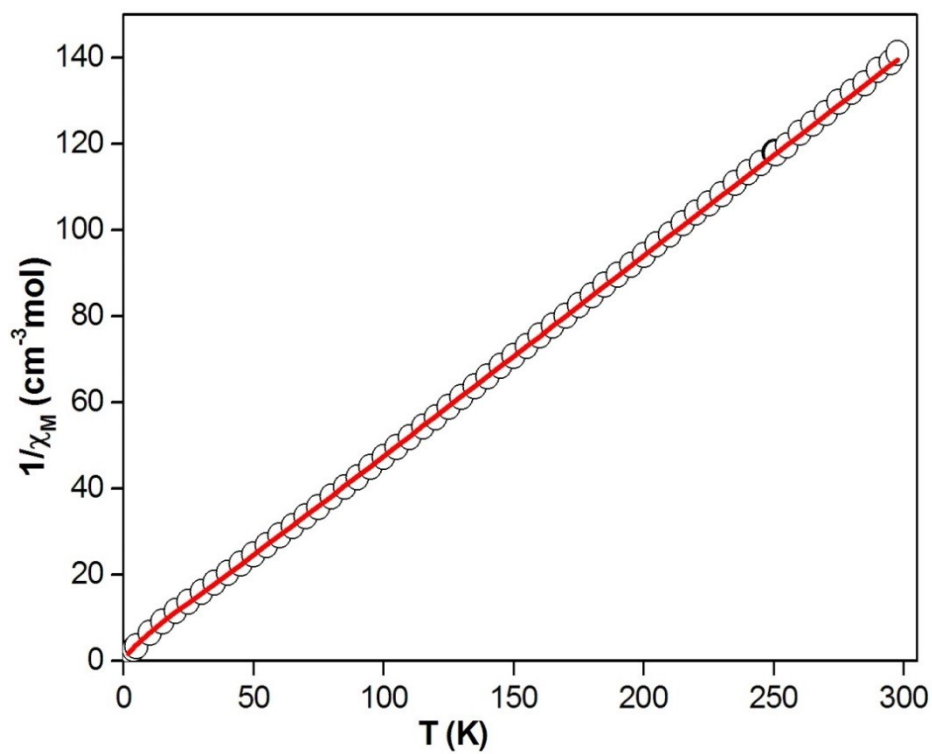


Figure S4. Variation of $1/\chi_M$ against temperature for **1**. Circles represent experimental value and the solid line represents the best fit obtained by using PHI program.

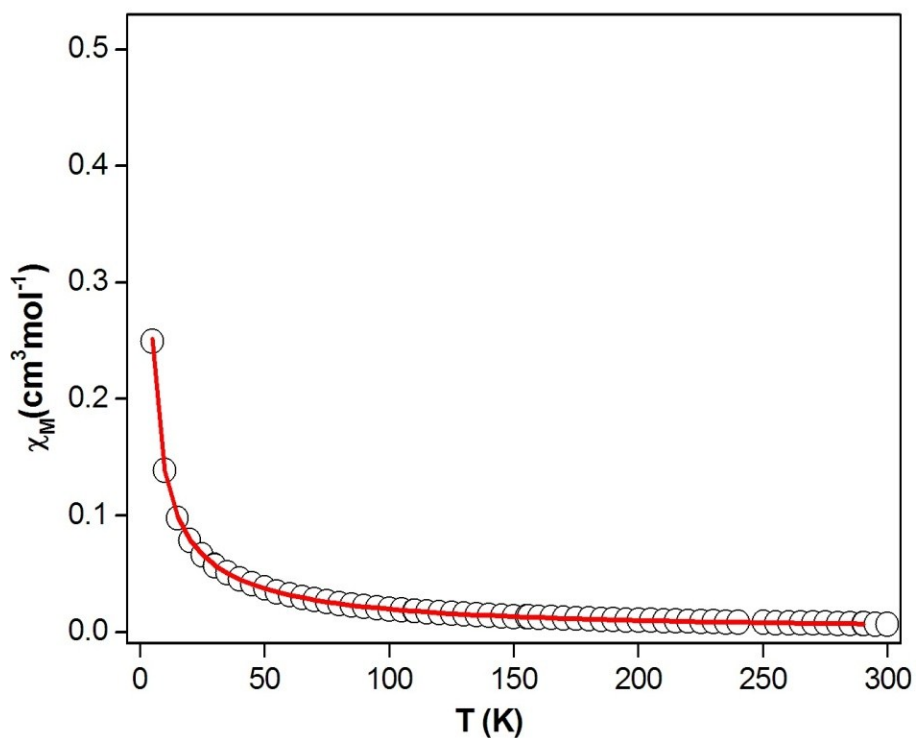


Figure S5. Temperature dependence of χ_M curve for **2**. Circles represent experimental value and the solid line represents the best fit obtained by using PHI program.

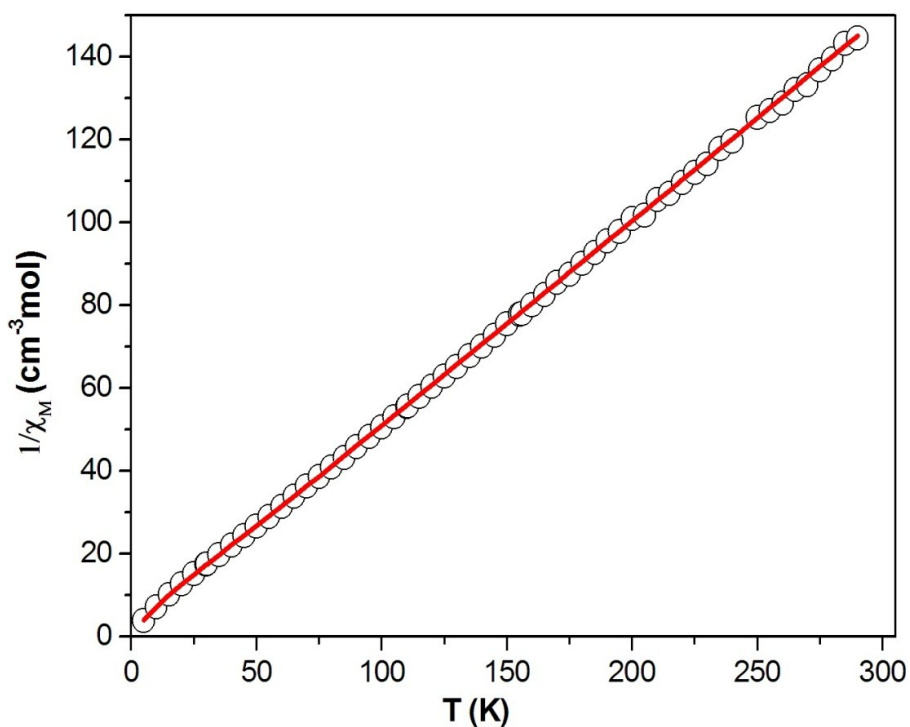


Figure S6. Variation of $1/\chi_M$ against temperature for **2**. Circles represent experimental value and the solid line represents the best fit obtained by using PHI program.

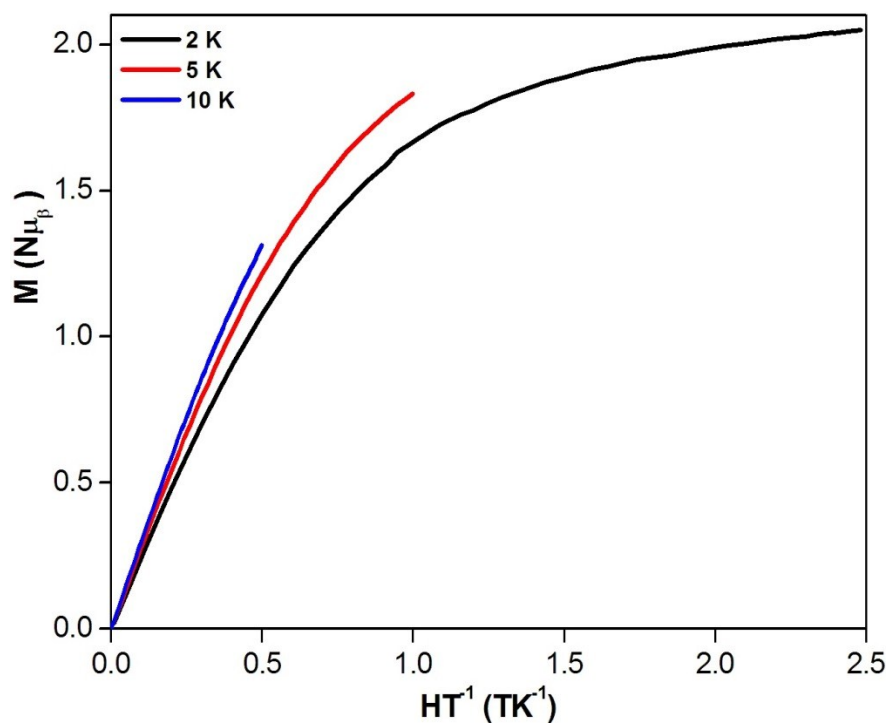


Figure S7. Reduced magnetization M versus HT^{-1} plot of 1.

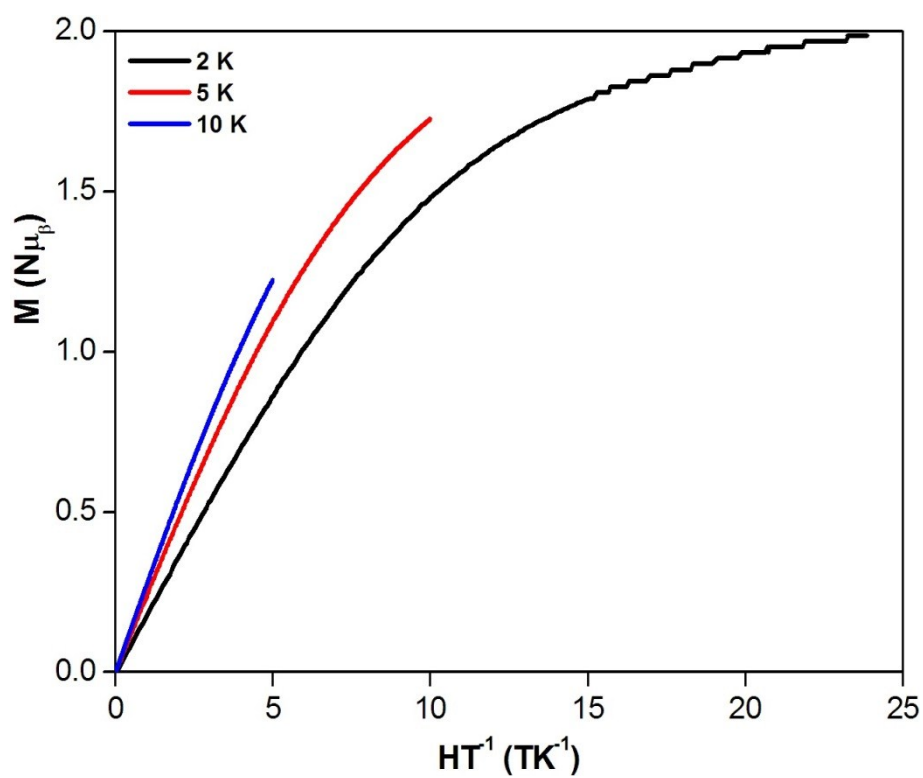


Figure S8. Reduced magnetization M versus HT^{-1} plot of 2.

References:

- [1] T. J. Giordano, G. J. Palenik, R. C. Palenik and D. A. Sullivan, *Inorg. Chem.*, **1979**, *18*, 2445.
- [2] C. Pelizzi, G. Pelizzi, S. Porretta and F. Vitali, *Acta Crystallogr. Sect. A Acta Crystallogr. Sec. C*, **1986**, *42*, 1131.
- [3] M. Villanueva, M. Urtiaga, J. L. Mesa and M. I. Arriortua, *Acta Cryst.*, **2004**, *E60*, m1175.
- [4] G. M. Sheldrick, *Acta Crystallogr., Sect. 64A*, **2008**, 112.
- [5] F. Neese (Max Planck-Institute for Bioinorganic Chemistry), *ORCA, Version 2.9.0*, January **2012**, An ab initio, DFT and semiempirical SCF-MO package –with contributions from U. Becker, D. Bykov, D. Ganyushin, A. Hansen, R. Izsak, D.G. Liakos, C. Kollmar, S. Kossmann, D.A. Pantazis, T. Petrenko, C. Reimann, C. Riplinger, M. Roemelt, B. Sandhöfer, I. Schapiro, K. Sivalingam, F. Wennmohs, B. Wezislá and contributions from collaborators: M. Kállay, S. Grimme, E. Valeev.
- [6] D. Andrae, U. Haessermann, M. Dolg, H. Stoll, H. Preuss, *Theor. Chim. Acta*, **1990**, *77*, 123.
- [7] A. Schafer, C. Huber, R. Ahlrichs, *J. Chem. Phys.* **1994**, *100*, 5829.
- [8] A. D. Becke, *J. Chem. Phys.* **1993**, *98*, 1372.